Diagnostics design for steady-state operation of the Wendelstein 7-X stellarator

Diagnostics design for steady-state operation of the Wendelstein 7-X stellarator[a)]

R. König,[1,b)] J. Baldzuhn,[1] W. Biel,[2] C. Biedermann,[1] R. Burhenn,[1] S. Bozhenkov,[1] J. Cantarini,[1] H. Dreier,[1] M. Endler,[1] H.-J. Hartfuss,[1] D. Hildebrandt,[1] M. Hirsch,[1] M. Jakubowski,[1] R. Jimenez-Gomez,[3] G. Kocsis,[4] P. Kornejev,[1] M. Krychowiak,[1] H. P. Laqua,[1] M. Laux,[1] J. W. Oosterbeek,[5] E. Pasch,[1] T. Richert,[1] W. Schneider,[1] B. Schweer,[2] J. Svensson,[1] H. Thomsen,[1] A. Weller,[1] A. Werner,[1] R. Wolf,[1] D. Zhang,[1] and S. Zoletnik[4]

[1]*Max-Planck-Institute für Plasmaphysik, EURATOM Association, Greifswald D-1749, Germany*
[2]*Forschungszentrum Jülich GmbH, EURATOM Association, Jülich D-52425, Germany*
[3]*CIEMAT, EURATOM Association, Avda. Complutense, Madrid 22-28040, Spain*
[4]*KFKI, RMKI, Association EURATOM, H-1121 Budapest, Konkoly Thege 29-33, Hungary*
[5]*Technische Universiteit Eindhoven, Den Doelch 2, 5612 AZ Eindhoven, The Netherlands*

(Presented 19 May 2010; received 17 May 2010; accepted 2 June 2010; published online 28 October 2010)

The status of the diagnostic developments for the quasistationary operable stellarator Wendelstein 7-X (maximum pulse length of 30 min at 10 MW ECRH heating at 140 GHz) will be reported on. Significant emphasis is being given to the issue of ECRH stray radiation shielding of in-vessel diagnostic components, which will be critical at high density operation requiring O2 and OXB heating. © *2010 American Institute of Physics.* [doi:10.1063/1.3483210]

I. INTRODUCTION

The development of the roughly 30 startup diagnostics for Wendelstein 7-X (W7-X) is progressing well. At the present development stage, work concentrates primarily on the in-vessel diagnostics and diagnostic components as well as on the device control diagnostics. Concerning the in-vessel components, most of the thermal shielding/cooling issues have been solved meanwhile, and we are now concentrating on solving the various issues connected with the high ECRH stray radiation levels expected during high density long pulse divertor operation. Even though this will rarely be an issue during the initial short pulse operation phase with the uncooled divertor, appropriate solutions for the quasistationary operation phase need to be found now. This is necessary because many components, such as cables, magnetic diagnostics, etc., are located behind water coolable wall structures, which will all be in place already at the start of the W7-X operation, albeit without being connected to the external cooling water supply yet. The early installation of the cooling structures, which are required for the long pulse operation phase of W7-X, will help shorten the time required to changeover to the fully cooled device. The changeover will start after the completion of the first two-year experimental program. In other cases, the shielding of diagnostics against ECRH stray radiation needs to be an integral part of the design, which cannot be added later on.

[a)]Contributed paper, published as part of the Proceedings of the 18th Topical Conference on High-Temperature Plasma Diagnostics, Wildwood, New Jersey, May 2010.

[b)]Author to whom correspondence should be addressed. Electronic mail: rlk@ipp.mpg.de.

II. ECRH STRAY RADIATION

At 2.5 T high density plasma operation above the X2 cutoff density of 1.25×10^{20} m^{-3}, nonabsorbed ECRH power densities of more than 20% are expected (Fig. 1). This stray radiation causes radiation flux densities at the walls of up to 200 kW/m^2 in the ECRH launching module and still about 20 kW/m^2 at the opposite side of the W7-X torus (using the experimentally determined average absorption coefficient across all in-vessel components in W7-AS of 15% as a first estimate). To investigate the effect of ECRH stray radiation on all in-vessel components, a water cooled aluminum test chamber (2.2 m long, 1.5 m diameter), the so-called Microwave Stray Radiation Launch (MISTRAL) (Ref. 1) facility has been set up, which can accept even the largest W7-X port plug-ins. The chamber is fed by a W7-X gyrotron operated at reduced power (200 kW). By varying the duty cycle of a train of short pulses of typically 5 ms duration, average power flux densities between 10 and 100 kW/m^2 can be set. A homogeneous stray field distribution within the central 0.9 m diameter cylindrical region is created by reflecting the power launched into the chamber via a corrugated waveguide and directing it, by a twofold mirror directly at the entrance port, poloidally along the chamber wall (inlet in Fig. 2). This directed radiation beam is multiply reflected along the chamber wall, creating a mantel of directed high beam power, within which a 0.9 m diameter core of isotropic radiation is formed solely by scattering of this radiation on the surface roughness of the vessel wall.[2]

Very helpful for understanding the distribution of the stray radiation in chambers, such as MISTRAL or W7-X, is to picture it like a collisionless gas in a container (molecular flow regime) and describe it as a multiresonator power bal-

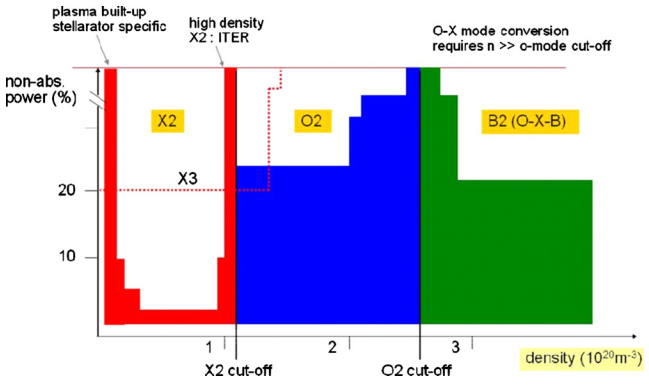

FIG. 1. (Color online) Expected nonabsorbed ECRH power vs plasma density.

ance for an ensemble of coupled cavities.[3] The reason for this analogy, to be fairly appropriate, is the large numbers of reflections of the ECRH stray radiation until final absorption due to the low absorption coefficients of most dominant in-vessel materials (typical values are Al: 0.006; stainless steel (SS): 0.026; and C: 0.05). The appropriateness of this analogy was clearly visible in an experiment to investigate the power density reduction along a 300 mm diameter, 1.7 m long port tube attached to and reaching into the isotropic region of the MISTRAL chamber: lining the inside of the SS port tube with a Sigraflex® carbon foil resulted in the same power density fall-off ratio along the tube as with pure Al chamber walls—but a significant reduction of the power density in the entire MISTRAL chamber including the port. This finding is in line with the added absorbing surface area with its high absorption coefficient (5%) compared to the one of the Al chamber walls (0.1%). This experiment demonstrates very clearly that reducing the ECRH stray radiation power density onto diagnostics components will either require a very diagnostic specific and individual shielding design or an overall reduction of the stray radiation level. The latter could only be achieved by coating large areas, e.g., the front and/or back side of the wall cooling panels or the plasma vessel (PV) wall, with a highly absorbing material, such as B_4C (d=300 μm: ~50%)[4] or Al_2O_3–TiO_2 (d=150 μm: ~80% absorption). This, however, is presently not foreseen for cost reasons. Following the experiments of the past months, the expected absolute power densities are almost less clear than

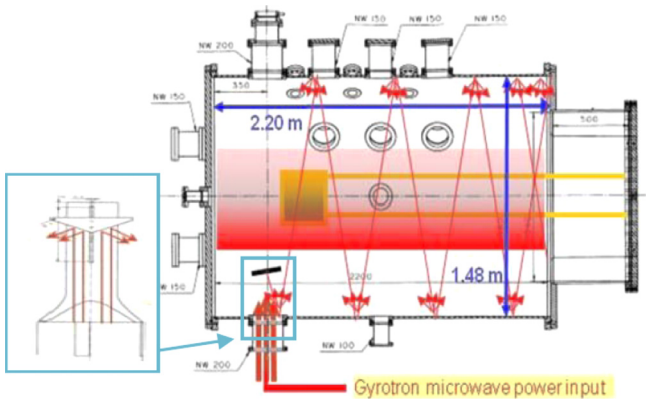

FIG. 2. (Color online) ECRH stray radiation test chamber MISTRAL.

before. It was found that with a typical skin depth of 1 μm, the surface roughness of any material exposed to the stray radiation has a strong effect on their effective absorption coefficient, i.e., they can be significantly larger than anticipated.[5] This effect was observed with new graphite bolometers for local measurements. These bolometers were developed to replace the sniffer probes that proved to be unsuitable for measurements on MISTRAL due to modes that could not be suppressed sufficiently by an added internal mode scrambler. For this reason, a silicone oil based detector is presently being developed at the University of Eindhoven, and special experiments to measure the absorption coefficients of the actual main in vessel material components of W7-X are being prepared.[2]

With respect to the diagnostics, all design measures possible are taken to reduce the impact of the ECRH stray radiation. In case of the magnetic diagnostics and general in-vessel cabling, complete enclosing by SS or Cu pipes seems unavoidable for most applications. Special measures are necessary if high time resolution is required.[5] Thermocoax® were found to be suitable for thermocouples, while minerally insulated twisted pair cables from the Japanese Okazaki Manufacturing Co. still need to be tested for their suitability for magnetic diagnostics. The widely used knitted wire meshes must be avoided for shielding since they strongly heat up due to their large surface and poor heat conductivity. As electrical breaks in beamlines of ex-vessel diagnostics, classical ceramic breaks cannot be used because of their strong microwave absorption. Instead, insulating PEEK® sealings, well shielded by labyrinth structures milled into the flange connection, have been designed. Diagnostics with an observation window at the air vacuum boundary, such as charge exchange recombination spectroscopy (CXRS), Thomson scattering, visible spectroscopy, etc., can be well shielded against ECRH stray radiation by coating them with an indium tin oxide (ITO) layer as suggested earlier on.[6] The company Melles Griot has developed a prototype of a 96 mm diameter, 12 mm thick Suprasil window with a low surface resistivity ITO film ($<10\ \Omega/\mathrm{cm}^2$, layer thickness of 1–1.5 μm, and maximum operating temperature in air of 270 °C), spectral transmission range (Fig. 3) suitable for the CXRS diagnostic, with excellent ECRH radiation blocking efficiency: 0.5% transmission at 140 GHz. Further windows optimized for other diagnostics and their specific spectral range requirements will be developed in the near future. In particular, a push toward increasing the transmission at the short wavelength end, to get access to the hydrogen Balmer series limit, is necessary. Earlier work has demonstrated the feasibility of this aim.[7] In some cases, the total integrated ECRH stray radiation power load (as well as the thermal power load from plasma radiation) on sensitive diagnostics components, such as windows or detectors, can be significantly reduced by observation through pinholes, like in the case of the toroidal video observation,[6] the IR/visible endoscopes for two-dimensional divertor temperature control and plasma symmetry investigations,[8] or the bolometer cameras.[5,9] In the last case, the detectors are additionally shielded by a cooled wire grid right in front of the detectors. For all these diagnostics, a fairly closed cavity forms be-

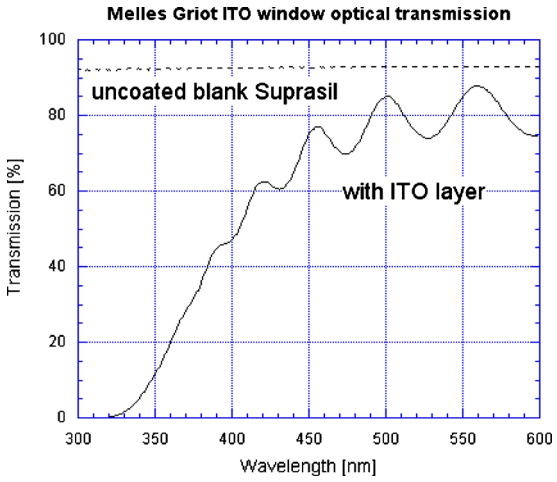

FIG. 3. (Color online) Optical transmission of an ITO coated ECRH stray radiation blocking window developed by Melles Griot GmbH.

tween the pinhole and the reflecting window or wire grid, making it essential to coat these cavity walls with a highly absorbing material. In case of the highly ECRH stray radiation sensitive bolometer, experiments in the MISTRAL chamber will soon show whether the absorbing surface needs to be increased by additional absorber coated lamellae.[9] The University of Stuttgart has recently developed a special $Al_2O_3-TiO_2$ coating for the water cooled Chevrons of our divertor cryopumps with an absorption of about 80%. Presently, the cavities of the bolometer and video diagnostic are being coated in preparation for tests in MISTRAL with an 87/13 material mix.

III. STARTUP DIAGNOSTICS DEVELOPMENT

A. Divertor diagnostics

Of the ten long pulse compatible IR/visible endoscope systems[8] for divertor temperature control and plasma symmetry investigations for all ten W7-X divertor modules, initially, i.e., during the uncooled divertor operation phase, only two systems will be installed, one looking at an upper and one at a lower divertor. The other eight systems will be replaced during the initial, short pulse operation phase of W7-X by a rather simplified version with the microbolometer IR and video/H_α cameras being mounted at the plasma facing end of the port tubes looking through windows equipped with uncooled shutters. A manufacturer for the microbolometer cameras (640×480 pixel) had been found (Dias Infrared GmbH), who was prepared to harden his systems for operation in strong magnetic fields. A camera has been tested successfully in the 3 T magnetic resonance tomograph at the Greifswald University clinic. Furthermore, every tenth target finger of all ten discrete divertors will be equipped with a thermocouple suitable for IR camera calibration during the cooling down phase of the target tiles directly after a pulse. This minimum number has been chosen such that for all magnetic field configurations, the island divertor strike lines will at least be located on one or two of them. Two rows of target integrated Langmuir probes with alternating probe tip locations in the two adjacent target fingers (alternating average tip to tip separation: 12.5 mm; radial tip width: 3 mm), to allow for better heat spreading in the material between the probe tips, have been developed and successfully tested in GLADIS at 8 MW/m^2 for 6.25 s (Fig. 4).

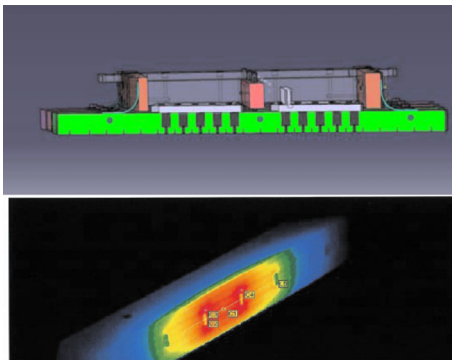

FIG. 4. (Color online) Top: flush mounted Langmuir probes. Tip to tip separation in one target finger 25 mm. Bottom: target exposed in GLADIS to 8 MW/m^2 for 6.25 s (blue: 400 °C; red: 1800 °C); start temperature: 200 °C.

A thermal He-beam beam nozzle box with five independent drivable piezovalves (spatial separation: 15 mm; gas pulse length 5 ms) connected to capillary "nozzle" tubes (inner diameter: 0.5 mm), which penetrate through a special narrow gap between two target fingers, has been designed such that it can be fitted to the actively water cooled divertor as well as the initial uncooled divertor. One upper and one lower divertor will be equipped with such an actively water cooled nozzle box at a toroidal location where spatially resolved spectroscopic observation will be available under 90°, i.e., parallel to the target plate, via the AEJ ports (Fig. 5). A Bayesian population model, including all levels up to and including n=5, has been developed and used to demonstrate that a thermal He-beam can even be used for n_e and T_e measurements of high density, low temperature divertor plasmas.[10] Figure 6 shows profiles of expected signals for a standard magnetic configuration EMC3/EIRENE simulation of a partially detached W7-X island divertor plasma. It was found that the plasma emission should be measurable in a region from about 10 to 30 mm above the target plates. With the standard line ratio technique for $n_e=1\times10^{20}$ m^{-3} and $T_e=5$ eV, the n_e and T_e errors, obtained from our probabilistic model, would be about 128% and 45%, respectively, for an assumed relative intensity measurement error of 5%. However, if instead of line intensity ratios, the absolute line intensities are measured and the ground level population are

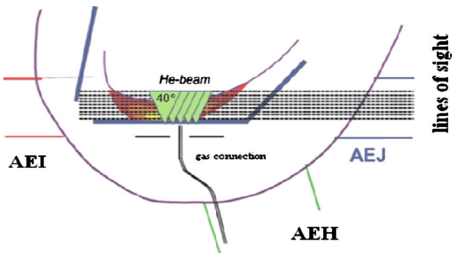

FIG. 5. (Color online) Five nozzle thermal He-beam injecting the gas through a narrow special diagnostic gap (maximum width: 10 mm) between two target tiles into the island divertor plasma.

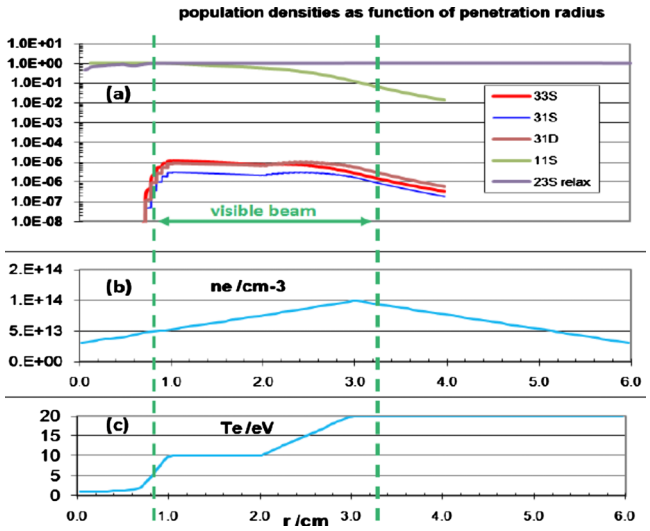

FIG. 6. (Color online) (a) Radial profiles of level populations relative to the initial ground level ($1\ ^1S$) population (the beam divergence is not accounted for). [(b) and (c)] Input profiles of plasma parameters from EMC3/EIRENE calculations.

derived, a considerable improvement in particular of the temperature measurement accuracy can be achieved. The ground level population can be determined by measuring the gas flow and the beam divergence in the laboratory and by calculating the beam attenuation stepwise from the measured n_e and T_e. The impact of the uncertainty in the beam attenuation has been assessed by treating it as a nuisance parameter in the probabilistic model with a normal distribution with a relative standard deviation of 50%. With this Bayesian model, we estimated the n_e and T_e errors to be 66% and 8% for 5% or 122% and 9% for 10% measurement errors, respectively. Including three more lines gives little improvement to 103% and 8%, again for an assumed 10% measurement error. This shows that a thermal He-beam can even for detached plasma conditions provide useful local plasma parameter information.

B. Core diagnostics

Significant progress has been made in the development of the two-color interferometer for density control, where a vibration compensation of a factor of 2000, corresponding to vibrations O(100 μm), has been demonstrated. Furthermore, the tests of four dispersion interferometer modules developed and manufactured by the Budker Institute in Novosibirsk, Russia, and presently envisaged for the W7-X multichannel interferometer have started at TEXTOR. The design of the two startup diagnostics cameras for the bolometer tomography system (later, more cameras will be added) is close to completion.[9] For the Thomson scattering diagnostic,[11] which initially will make use of two (later 5) Q-switched Nd:YAG (YAG denotes yttrium aluminum garnet) 1.5 J lasers (laser frequency of 20 Hz), all optical components required for the startup phase have been designed (Fig. 7). An eight-lens system, f/1.3 [numerical aperture (NA)=0.37], 160 mm diameter, f=172 mm, 16 kg, with a titanium housing suitable for operation at temperatures between 20 and 200 °C, has been designed and is presently being manufactured by the company Sill Optics. Twenty-seven Quartz fiber bundles, covering a plasma half profile (spatial resolution of 2.5 cm), with matching NA of 0.37 and rectangular cross section (three combined bundles of 0.9×3.7 mm^2 of different length, delay line) at the plasma facing end and 3 mm diameter circular cross section at the other end, transports the light to initially nine (later 30) polychromators. The polychromators again have a matching NA of 0.37. They have been optimized for the plasma parameter ranges: 20 eV$<T_e<$10 keV and 5×10^{18} m$^{-3}<n_e<5\times10^{20}$ m^{-3}. The widths of the five interference filters (one for Raman calibration at N_2) have been suitably chosen for this parameter range (Fig. 8). The expected performance has been successfully confirmed with a prototype polychromator at the ASDEX Thomson scattering system and a full series production has been started at the Institute of Nuclear Physics, Cracow, Poland. As detectors, silicon avalanche diodes (PerkinElmer) are being used, which have a matching diameter of 3 mm.

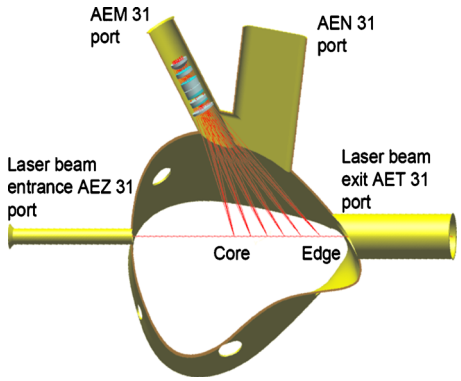

FIG. 7. (Color online) Thomson scattering diagnostic: the laser beam is launched through the AET–AEZ ports. Observation of the outer half radius from AEM port, the observation optic for the inner half radius will later be installed in the AEN port. The common water cooled shutter for both ports is driven via the AEN port.

For the high efficiency extreme ultraviolet overview spectrometer system,[5] covering the spectral range from 2.5 to 160 nm, which is in test operation on TEXTOR, the support frame for W7-X has been designed, which also required to move the four turbo pumps far back into the region where the magnetic stray field is less than 5 mT. For the active charge exchange neutral particle analysis (CX-NPA) system, consisting of two 24 energy channel ACORD systems

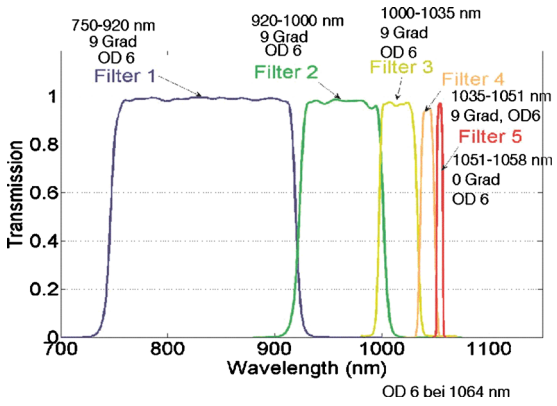

FIG. 8. (Color online) Filter widths of the Thomson polychromators.

(0.3–80 keV) and one 27 channel compact C-NPA (0.6–60 keV) looking at the W7-X diagnostic neutral beam, the mechanical support structure has been designed. The systems can be moved between pulses and can cover the central half of the plasma with each having a spatial resolution of about 5 cm. Measurements with an ACORD system on MAST and in a Helmholtz coil setup of W7-A coils have shown the need of magnetic shielding for the detectors at which W7-X would be exposed to 10 mT at their installation location.[12]

[1] S. Ulrich, H.-J. Hartfuss, M. Hirsch, and H. Laqua, Stellarator News **98**, 1 (2005).
[2] M. Hirsch, J. W. Oosterbeek, R. Jimenez, J. Baldzuhn, M. Endler, M. Laux, D. Zhang, H. P. Laqua, F. Noke, F. Purps, K. Ewert, and W7-X Team, Proceedings of the International Conference on Plasma Diagnostics, Pont-à-Mousson, France, 12–16 April 2010.
[3] H. Laqua, V. Erckmann, M. Hirsch, W7-AS Team, and F. Gandini, Proceedings of the 28th EPS Conference on Controlled Fusion and Plasma Physics, Madeira, 18–22 June 2001, Vol. 25A, pp. 1277–1280, P3.099.
[4] Max-Planck-Institute for Plasma Physics Annual Report 2003, University of Stuttgart Contributions, p. 100.
[5] R. Burhenn, J. Baldzuhn, W. Biel, H. Dreier, M. Endler, R. Jimenez-Gomez, K. Grosser, H. J. Hartfuss, D. Hildebrandt, M. Hirsch, R. König, P. Kornejev, M. Krychowiak, H. P. Laqua, M. Laux, J. W. Oosterbeek, E. Pasch, W. Schneider, H. Thomsen, A. Weller, A. Werner, R. Wolf, and D. Zhang, "Diagnostics development towards steady state operation in fusion devices," presented at International Conference on Plasma Diagnostics, Pont-à-Mousson, France, 12–16 April 2010 [Contrib. Plasma Phys. (to be published)].
[6] R. König, J. Cantarini, H. Dreier, V. Erckmann, D. Hildebrandt, M. Hirsch, G. Kocsis, P. Kornejew, M. Laux, H. Laqua, E. Pasch, S. Recsei, V. Szabo, H. Thomsen, A. Weller, A. Werner, R. Wolf, M. Y. Ye, and S. Zoletnik, Rev. Sci. Instrum. **79**, 10F337 (2008).
[7] S. Ray, R. Banerjee, N. Basu, A. K. Batabyal, and A. K. Barua, J. Appl. Phys. **54**, 3497 (1983).
[8] J. Cantarini, D. Hildebrandt, R. König, F. Klinkhamer, K. Moddemeijer, W. Vliegenthart, and R. Wolf, Rev. Sci. Instrum. **79**, 10F513 (2008).
[9] D. Zhang, R. Burhenn, R. Koenig, L. Giannone, P. A. Grodzki, B. Klein, K. Grosser, J. Baldzuhn, K. Ewert, V. Erckmann, M. Hirsch, H. P. Laqua, and J. W. Oosterbeek, Rev. Sci. Instrum. **81**, 10E134 (2010).
[10] M. Krychowiak, M. Brix, D. Dodt, Y. Feng, R. König, O. Schmitz, J. Svensson, and R. Wolf, "Bayesian modelling of a thermal helium beam for measurement of electron density and temperature in the W7-X divertor plasma," presented at International Conference on Plasma Diagnostics, Pont-à-Mousson, France, 12–16 April 2010 [Plasma Phys. Contr. Fusion (to be published)].
[11] J. Cantarini, J. P. Knauer, and E. Pasch, AIP Conf. Proc. 993, 192 (2007).
[12] W. Schneider, M. R. Turnyanskiy, V. I. Afanasyev, F. V. Chernyshev, and T. Richert, Proceedings of the 37th International Conference on Plasma Diagnostics, Dublin, Ireland, 21–27 June 2010.